



UNIVERSITI  
TEKNOLOGI  
MARA



# Globalising Knowledge and Information

## SCIENCE TECHNOLOGY

## NATIONAL SEMINAR ON

## SCIENCE TECHNOLOGY & SOCIAL SCIENCES

## 2006

30-31 May 2006

Swiss Garden Resort & Spa  
Kuantan, Pahang





## Implementation of a Ray Tracing Simulator for Propagation Prediction

P.Thirumaraiselvan

### ABSTRACT

*In wireless communications, understanding of the propagation channels is necessary to achieve optimum performance of a communication system. Even though direct measurements enable accurate evaluation of onsite performance, it requires a considerable amount of time and efforts. Therefore, a computer tool that could characterize the wireless channel from the building plans and material properties would be a good solution. This paper considers an approach for developing such a simulation tool using ray tracing. The simulator has been implemented in Matlab. Assuming that the scattering objects are much larger than the wavelength, the electromagnetic waves are modelled as rays. From the ray tracing results, received field strength is computed based on the theory of Geometrical Optics and Uniform Geometrical Theory of Diffraction.*

**Keywords:** Ray tracing simulation, propagation prediction, Geometrical Optics, Uniform Geometrical Theory of Diffraction

### Introduction

In indoor or outdoor microcellular communication system, if the volume of the users exceeds the limit, the cell size of the transmitting base station needs to be optimized to accommodate the increased spectrum requirement. At the same time care should also be taken to minimize the region of poor coverage and the overlapped areas. The above objectives are feasible only with the propagation study in such environments. Due to the reflection, transmission and scattering of the radio waves by structures inside a building or in city streets, the transmitted signal reaches the receiver by more than one path. This multipath propagation causes inter symbol interference in a wireless communication system. Besides this the interference between the signals from the co-channel cells, co-channel interference, also reduces the performance of a wireless system. Even though these interferences are often generated within the cellular system, they cannot be completely eliminated. However if the channel is characterized well, the effective transmitter antenna locations can be selected such that optimum propagation performance will be achieved. This requires the use of propagation prediction tools, since direct measurements are not cost effective.

This paper considers a method to make such a tool and the shoot-and-bounce ray tracing technique(SBR) is implemented to predict the path of reflected and transmitted rays (Seidel & Rappaport 1994). It also includes single diffraction from the diffracting edges. The field intensity at the receiver with respect to the reference field strength, i.e. at 1m from the transmitter, due to the reflected, transmitted and diffracted signal components is computed with geometrical optics and uniform geometrical theory of diffraction. This field intensity can be further used to get the desired parameters, such as path loss and RMS delay spread, for channel estimation and cell planning.

### Shoot and Bounce Ray Tracing

In SBR method, from the transmitter, the rays are launched in all directions and the progress of each ray is traced through the environment, taking into account the propagation mechanisms. For each ray, intersection tests are conducted between ray and obstacles. At every intersection point, a ray is split into a reflected ray and transmitted ray. Before conducting the intersection test for these two rays, a reception test is performed on them. The ray tree in Figure 1 shows, how a source ray can be decomposed into many transmitted and reflected rays due to the intersections with planer boundaries. To test whether a ray is received or not, a reception sphere is constructed about the receiver. If the ray intersects the reception sphere, it is considered as received. The radius of the above mentioned reception sphere is an important one. It should be sized to guarantee the reception of one and only one ray from each wave front (Durgin, Patwari & Rappaport 1997). This ray tracing is done until a maximum number of scattering levels is exceeded or has no further intersection. The distance travelled, direction of arrival and phase are recorded to compute the field intensity later.

### Ray Tracer

Before performing ray tracing, the ray tracer checks whether the receiver is visible from the transmitter position, i.e. for line-of-sight path. At first, ray-object intersection test is performed with a ray that goes through the receiver from

the transmitter and the object intersection distance is found. If there are no obstacles between them, the object intersection distance will be zero or greater than the distance between the transmitter and receiver. Then, the electric field intensity due to the direct ray is calculated. Next, the rays are launched from the transmitter and the SBR ray tracing technique is applied to compute all the reflection points and the direction vectors of reflected rays; the ray direction vectors that are derived in the previous section are used to launch the rays. At first, a source ray is taken and intersection test is performed to find the point of intersection/reflection. If there is no reflection from the obstacles, i.e. if there is no intersection, the ray is dropped; with a new ray, the ray tracing is continued. From every point of reflection a reception test is performed. If the ray is received, the reflecting objects/planes in that propagation path, reflection levels and the total distance travelled are recorded. Then with these details, the brute force double ray counting verification is carried out (Flores, Mayorgas, Jimenez 1998). That is, the reception is considered only if there is no previous ray that follows the same path. Then field intensity is computed for the received ray. Upon reflection, the source ray is divided into a transmitted ray and a reflected ray. Ray tracing is preceded with the direction vectors of these two rays separately. Direction vector of the incident ray is used as that of the transmitted ray with the intersection point as its origin. This recursive, ray-tracing procedure is continued until it reaches a maximum number of tree levels. The direct diffraction is also incorporated in this ray-tracing simulator and the field intensity of the received rays due to diffraction is determined next. Finally, the vector sum of all the received field components is obtained and used to determine the path loss.

### Total Electric Field Intensity at the Receiver

Due to multipath propagation, the number of rays received by the receiver is often more than one; that is direct, reflected, transmitted and diffracted rays. Hence, the total electric field intensity,  $E_r$ , is obtained by the coherent summation of individual ray contribution. The complex field intensity of  $m^{th}$  ray, which experiences multiple reflection and transmission, at the receiver is given by (Seidel & Rappaport 1994)

$$E_m = E_i(Q_m) \prod_{n=1}^x A_{nm} \Gamma(\theta_{nm}) \prod_{p=1}^y A_{pm} T(\theta_{pm}) e^{-jkd} \tag{1}$$

where

$E_i(Q_m)$  = Incident electric field intensity at the first scattering point,  $Q_m$

$\Gamma(\theta_{nm}), T(\theta_{pm})$  = associated reflection and transmission coefficients, respectively.

$A_{nm}, A_{pm}$  = spreading factors for reflection and transmission of the  $m^{th}$  multipath component, respectively

$d$  = total path length of  $m^{th}$  ray

$e^{-jkd}$  = propagation phase factor due to path length

$x, y$  = total number of reflections and transmissions, respectively

Since the diffraction is treated separately (single diffraction), the field intensity due to  $n^{th}$  diffracted ray at the receiver can be obtained by replacing the product of complex reflection and transmission coefficients in the equation 1 with the complex diffraction coefficient; that is

$$E_{dn} = E_i(Q_n) A_{dn} D_n e^{-jkd} \tag{2}$$

where,

$E_i(Q_n)$  = Incident electric field intensity at the diffraction point,  $Q_n$ , of  $n^{th}$  diffracted ray

$A_{dn}$  = spreading factor for  $n^{th}$  diffracted ray

$D_n$  = diffraction coefficient for  $n^{th}$  diffracted ray

$d$  = total path length of  $n^{th}$  diffracted ray

The total field intensity,  $E_r$ , due to all the received rays is

$$E_r = \sum_{m=1}^n E_m + \sum_{n=1}^z E_{dn} \tag{3}$$

where,

$n$  = total number of rays traced in the ray tracing part  
 $z$  = total number of diffracted rays

**Path Loss**

If the gains of the transmitter and receiver antennas are unity, the total received power can be defined as

$$P_r = P_t \left( \frac{\lambda}{4\pi} \right)^2 \left| \frac{E_r}{E_0} \right|^2 \tag{4}$$

where,

$P_t, P_r$  = transmitted and received power respectively  
 $E_r$  = total electric field intensity at the receiver

$E_r/E_0$  can be obtained from the total field intensity; that is from equation 3. The path loss is defined as the difference between the effective transmitted power and the received power in decibels (Rappaport 2002); that is

$$PL \text{ in dB} = 10 \log_{10} \left( \frac{P_t}{P_r} \right) = -20 \log_{10} \left( \frac{\lambda}{4\pi} \left| \frac{E_r}{E_0} \right| \right) \tag{5}$$

**Comparison with Two Ray Model**

To validate the ray tracer, a two-ray model is simulated and the results are compared with the results of Xia, Bertoni, Maciel, Stewart and Rowe (1993). The geometry for a two-ray model is shown in Figure 2. The antennas are assumed isotropic. The transmitting and receiving antenna heights are 8.7m and 1.6m respectively. The frequency of the incident wave is 900MHz. The receiver will receive one direct ray and one ground reflected ray. Received power for vertical and horizontal polarization is plotted against the antenna separation (shown in Figure 3). As the antenna separation increases, the path loss oscillates due to the interference between the two rays as they go in and out of phase. In addition, the received power reduces with the square of the antenna separation,  $d^2$ . At larger distances, it falls off with  $d^4$  (Rappaport 2002, chapter 4). Exact match with the results of Xia, Bertoni, Maciel, Stewart and Rowe (1993) is found in the shorter distances up to a few hundred meters. Slight deviation is noticed at longer distances and this is due to the increased radius of the reception sphere.

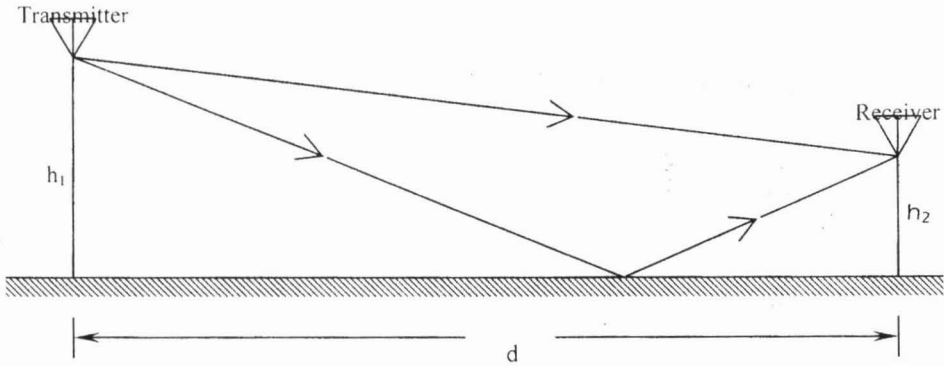


Fig. 2: Two Ray Model for Propagation above Flat Earth

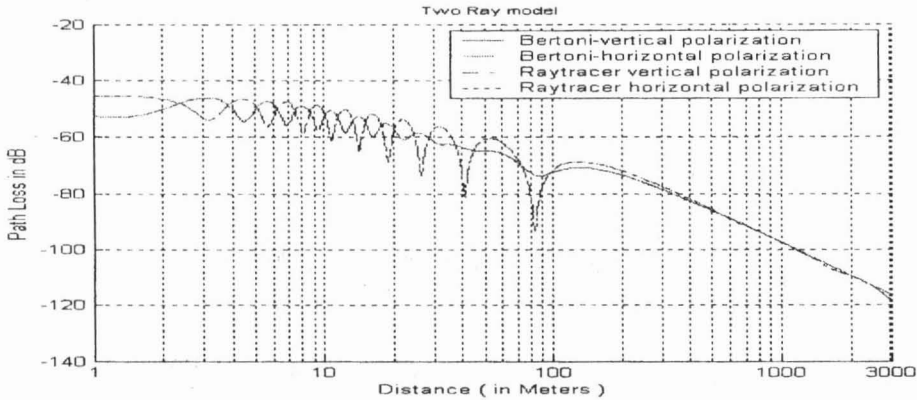


Fig. 3: Path Loss of the Two Ray Model

### Comparison with Measurements and Predictions in Ottawa City Streets

For further validation of the wave propagation prediction tool and to check its applicability to complex environments, path loss predictions for Ottawa city Streets environment are carried out and compared with the published measurements that have been collected at 910MHz in Ottawa City, Canada by Whitteker (1988) and with the simulation results of Tan and Tan (1995). The transmitter and receiver antennas used for the measurements were vertical monopoles. They were located on small ground planes at a height of 8.5m and 3.65m respectively. The measured data were recorded and path loss was plotted with 2m resolution. Each point was the median of the path loss samples, which were taken in 2m interval. The antenna gains were not included in the published measurements. The plan view of the simulated street scene is shown in Figure 4. The buildings are higher than the transmitting and receiving antennas and all the walls are assumed to have a dielectric constant ( $\epsilon_r$ ) 7.0 and conductivity ( $\sigma$ ) 0.2 S/m (Tan & Tan 1995). In this simulation, the transmitting and receiving antennas are modelled as Hertzian dipoles with unity gain. The received field strengths are predicted at random interval and used to compute the path losses. Up to ten reflections and single diffractions from diffracting corners are included; transmission mechanism is excluded from this prediction. Following Tan and Tan (1995), Fresnel reflection coefficients are used instead of the multi-layer wall reflection coefficients. The tessellation frequency of the transmitter icosahedron,  $N$ , is fixed at 172 so that the ray separation would be about 0.4 degrees.

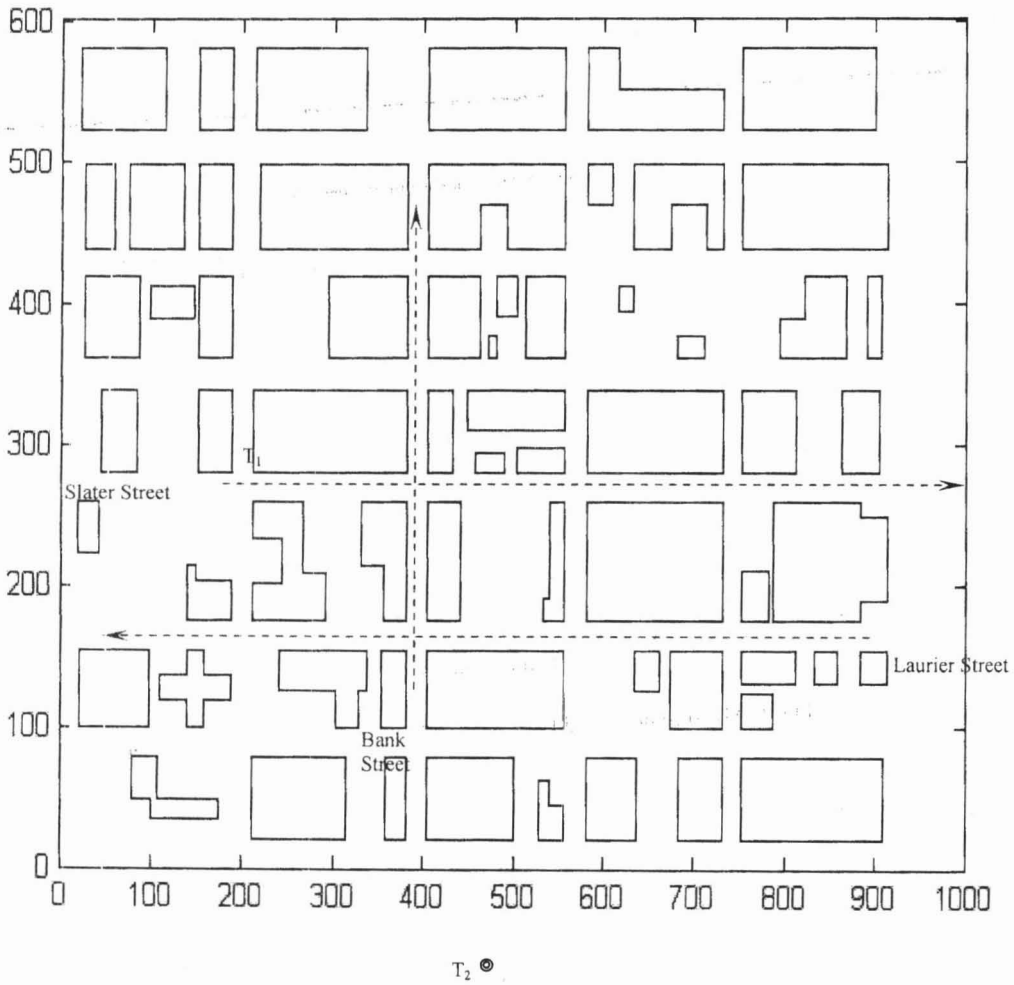


Fig. 4: Two Dimensional View of Ottawa City

At first, transmitter is placed at the Slater Street i.e. at  $T_1$ . Receiving antenna is moved along the Laurier Street. The path losses are predicted using the ray tracing simulator and plotted in Figure 5. Next, the transmitter is located at Laurier Street i.e. at  $T_2$ . The receiver is moved along the Bank Street. The path loss characteristics of this scenario are plotted in Figure 6. The measurements of Whitteker (1988) and the simulation results of Tan and Tan (1995) are also included for comparison in the Figures 5 and 6. Reasonable agreement found in these results ensures the validity of the simulator to some extent.

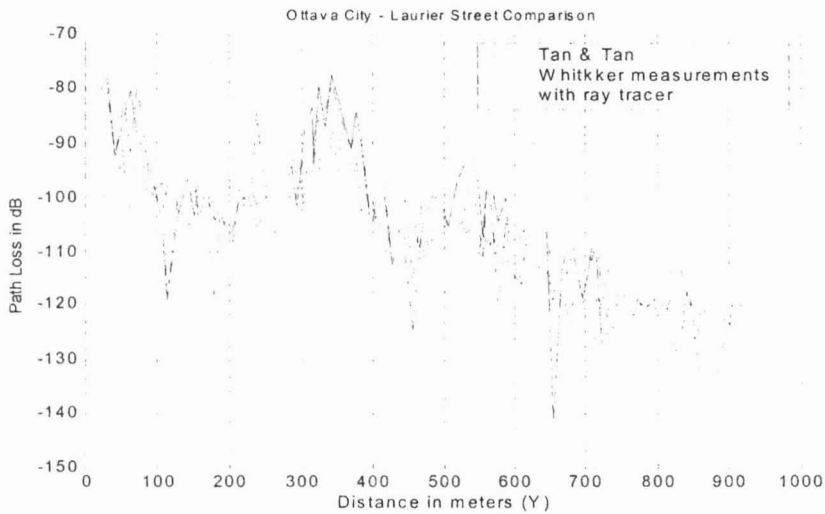


Fig. 5: Measurements and Predictions of Path Loss along Laurier Street

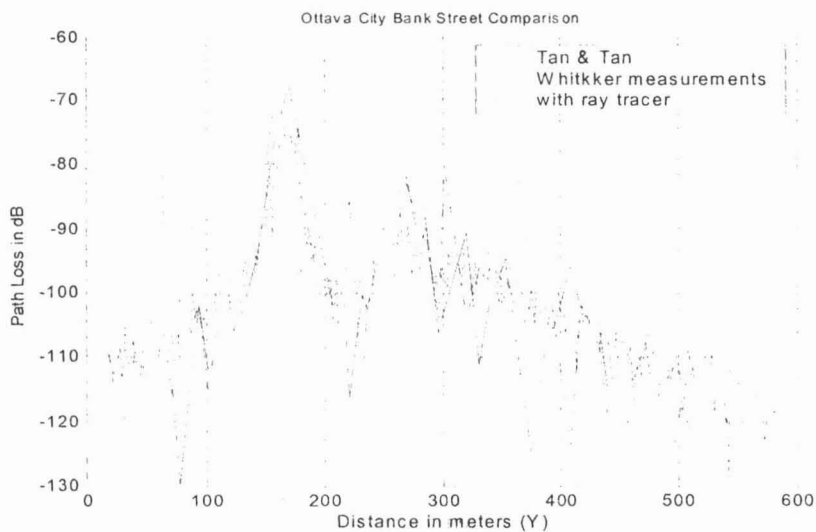


Fig. 6: Measurements and Predictions of Path Loss along Bank Street

### Conclusion

In this paper a ray tracing simulator, which can be used for wave propagation prediction of an indoor or outdoor microcellular communication system, has been discussed. This simulator can handle multiple reflections, transmissions, and combinations of them with the three dimensional shoot-and-bounce ray tracing technique. From the ray tracing results, received field strength is computed based on the theory of Geometrical Optics. In addition, single diffraction from diffracting corners and edges are included whereby the received field strength is determined using the Uniform Geometrical Theory of Diffraction. To validate the ray-tracing simulator, simulated results are compared with published measurements and predictions. Reasonably good agreement is observed.

## References

- Flores, S.J., Mayorgas, L.F., & Jimenez & F.A. (1998). Reception Algorithms for Ray Launching Modelling of Indoor Propagation. *RAWCON'98 Proceedings*: pp. 261-264.
- Keller, J.B. (1962). Geometrical Theory of Diffraction. *J. Opt. Soc. Am.*, vol. 52: pp. 116-130.
- Kouyoumjian, R.G., & Pathak, P.H. (1974). A Uniform Geometrical Theory of Diffraction for an Edge in a Perfectly Conducting Surface. *Proc. IEEE*, vol. 62, No. 11: pp. 1448-1461.
- McNamara, D.A., Pistorius, C.W.I. & Malherbe, J.A.G. (1990). *Introduction to the Uniform Geometrical Theory of Diffraction*. Boston: Artech House.
- Rappaport, T.S. (2002). *Wireless Communications Principles and Practice*. New Jersey: Prentice Hall.
- Seidel, S.Y., & Rappaport, T.S. (1994). Site-Specific Propagation Prediction for Wireless in-Building Personal Communication System Design. *IEEE Trans. Veh. Technol.*, vol. 43, No. 4: pp. 879-891.
- Tan, S.Y., & Tan, H.S. (1995). Propagation Model for Microcellular Communications Applied to Path Loss Measurements in Ottawa City Streets. *IEEE Trans. Veh. Technol.*, vol. 44, No. 2: pp. 313-317.
- Whitaker, J.H. (1988). Measurements of Path Loss at 910 MHz for Proposed Microcell Urban Mobile Systems. *IEEE Trans. Veh. Technol.*, vol. 37: pp. 125-129.
- Xia, H.H, Bertoni, H.L., Maciel, L.R., Stewart, A.L., & Rowe, R. (1993). Radio Propagation Characteristics for Line-of-Sight Microcellular and Personal Communications. *IEEE Trans. Antennas Propagat*, vol. 41: pp. 1439-1447.
- 

P.THIRUMARAISELVAN, Faculty of Electronics, Kolej Tafe Seremban.